PAPER REF: 3968

APPLICATION OF MULTIAXIAL HIGH-CYCLE FATIGUE CRITERIA IN ANALYSIS OF ROLLER BEARINGS

Paweł Romanowicz
Institute of Machine Design, Cracow University of Technology, Cracow, Poland
Email: promek@mech.pk.edu.pl

ABSTRACT

The rolling contact fatigue (RCF) calculations of spherical and roller bearings using multiaxial high-cycle fatigue criteria (MHCF) based on different approaches are presented in the work. In this case, the complex and non-proportional stress state with pulsating three dimensional compression occurs. Due to this fact, the level of fatigue effort was estimated by versions of hypotheses proposed by: Crossland, Dang Van, Papadopoulos, Łagoda. Numerical calculations were made using the finite element method – ANSYS. Results demonstrated that not all criteria proposed in literature for the RCF analysis gave correct results. The detailed analysis of influence of roller element and rings radii at the contact stress distribution is also presented.

Keywords: rolling contact fatigue, roller bearings, multiaxial high-cycle fatigue criteria, FEM.

INTRODUCTION

Ball and roller bearings are among the most important machine elements. They are used to allow rotary motion of the rotating parts and support significant loads. Due to the cyclic contact stresses, elements of rolling bearings are subjected to the rolling contact fatigue (RCF). This phenomenon is one of the main failure form of ball and roller bearing. Generally, the RCF is associated with a localized damage process of machine elements (railway wheels and gears [2, 27]) working in rolling contact conditions produced by cyclic contact loading. Fatigue failure is a result of cumulative process consisting of crack initiation, short and long crack growth and final fracture. This phenomenon is very dangerous, because the failure can occur in machine elements as the equivalent stress is below the yield point. Moreover, the single cycles of load would not produce any ill effects.

The two most dominant RCF mechanisms in rolling bearings are surface pitting and subsurface spalling. The pitting cracks initiate at the surface irregularities and grow from there into the material [29]. Initiation of such cracks is induced by pressing the lubricant into the gap, which in consequence leads to an increase of pressure in the gap and further crack propagation. Finally, after certain number of load cycles, a part of material break away.

In the second case, the subsurface fatigue cracks appears immediately below the load carrying surface where the largest shear stress amplitude occurs or in points in which the structure of the material is weakened (e.g. by non-metallic inclusions). In the next stage, the cracks extend up to surface and after that it forms the surface crack. Moreover, edges of damaged material are initiators of further cracks. This phenomenon progressively increases and eventually makes the bearing unserviceable. The continued operation of such damaged bearing can leads to an increase of noise, vibration and dynamic loads, and finally to complete failure. Generally, the inner-rings are more exposed at the fatigue failure than the rolling elements. It can be explained by the fact that the rolling elements are subjected to a more even fatigue loads.

In rolling contact the localized concentration of complex and multiaxial stresses occurs a few millimeters below the surface in a very small volume of element [8] and is extremely high in comparison with stresses in supported rotating machine elements. Moreover, the out-of-phase three dimensional pulsating large compressive and shear stresses occurs in the dangerous points [24]. Because of this, the principal axes constantly change their direction during a stress cycle. It should be noted that such multiaxial character of loading is absent in classical fatigue tests. Because of this, the fatigue life of rolling bearings cannot be investigated using classical fatigue models such as Smith's or Haigh's diagrams, which does not take into account the influence of non-proportional stresses at fatigue strength. Another specific issues of this phenomenon can be found in Ref. [6].

In the process of sub-surface RCF failure the amplitudes of stresses have a dominant role [27]. Therefore, in case of free rolling three characteristic points can be observed below the contact surface (Fig. 1). One of them is the Bielayev point (B), in which the equivalent von Mises stress achieves the highest value. This point is the most dangerous in the case of static contact (without rolling) of bodies loaded by cyclic forces. In the other Palmgren-Lundberg points (P-L), the shear stress τ_{xy} achieves the extreme values. In the case of free rolling or rolling with small friction coefficient, these shear stresses have equal absolute values but they have different sign. Because of this, the maximal amplitude of shear stress τ_{xy} occurs at the radius of P-L points ($r_{P\text{-}L}$) and these two points are the most dangerous in the repeated rolling contact [27].

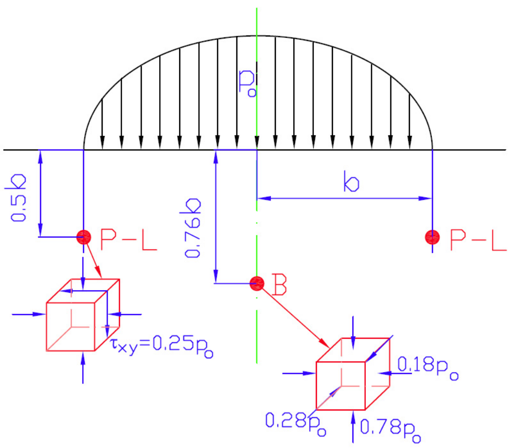

Fig.1 The location of the most dangerous points below the contact surface in the case of two infinitive cylinder pressed together, B is the Bielayev point, P-L are the Palmgren-Lundberg points.

The different models for rolling contact fatigue analysis of rolling bearings can be classified into two groups - probabilistic engineering life prediction models and deterministic research models. The first one, engineering models are very often formulated as empirical. In such formulas the variables are obtained from expensive experimental tests. As the example, the first and very popular in industry the probabilistic basic rating life model, based on probability of subsurface crack initiation formulated by Palmgren and Lundberg [15]:

$$L_{10} = \left(\frac{C}{P}\right)^{k}, \quad (1)$$

where L_{10} – basic rating life in million revolutions for 10% probability of failure, C – bearing basic dynamic load rating, P – equivalent load on the bearing, k – exponent of rolling bearing type (k=3 for ball bearing, k=10/3 for roller bearing).
The predicted life from the above equation is based on experimental tests of rolling bearings analyzed statistically. It was also assumed that subsurface cracks initiate due to the simultaneous occurrence of a weak point in the material and the maximal orthogonal shear stress. Other probabilistic criteria were proposed by (i) Ioannides and Harris [10], in which different stress measure (e.g. the von Mises stress, the maximal shear stress) were used, (ii) Schlicht et al. [30], which is the modification of (1) and have form:

$$L = a_1 \cdot a_{23} \cdot f_t (C/P)^k , \qquad (2)$$

where a_1 is the ISO factor for reliability, a_{23} is the adjusts for operating conditions, f_t is the adjusts for the loss of hardness at higher operating temperatures,
(iii) Shimizu [31], which proposed additional parameter known as minimum life prior to failure. The detailed descriptions of all probabilistic models can be found in Ref. [29].

The current ISO methods for calculation of rolling bearings [12] are based at the simplest method for basic rating life proposed by Palmgren-Lundberg (1) and modified rating life written in the following forms:

$$L_{n,\mathrm{m}} = a_1 \cdot a_{ISO} \cdot L_{10} , \qquad (3)$$

or

$$L_{n,\mathrm{m}} = a_1 \cdot a_2 \cdot a_3 \cdot L_{10} , \qquad (4)$$

where a_1 is the modification factor for reliability, a_{ISO} is the life modification factor, a_2 is the material and processing factor and a_3 is the application factor.
The above ISO standard (3, 4) is based on works published by Ioannides and Harris [10] and Ioannides et al. in 1999 [11]. As the fatigue limit the Von Mises stress of 900 MPa was used (it corresponds to a maximum Hertz contact stress of 1500 MPa). Moreover, it assumes that the bearing is made from AISI 52100 bearing steel and that the bearing is lubricated with mineral oil. However, it was observed that the high hardness bearing steel does not have any fatigue limit [31, 15-16]. Due to this fact, some critical remarks concerning assumptions of fatigue limit for AISI 52100 bearing steel in ISO 218 standard can be found in literature.

It can be observed, that such models does not directly consider the details of the constitutive behavior of material under repeated rolling contact. They can also have some limitations, i.e. P-L model (1) does not include the possibility of initiation cracks at the lubricated surface or assumptions (i.e. pure rolling contact without friction effects).

The second methods of bearing life calculation are based at deterministic research models and require complete information about $\sigma-\varepsilon$ material behavior response for contact problems. They are used in conjunction with a material failure models, such as crack initiation or crack propagation. The most widely used deterministic models based at plastic strain accumulation in strain hardening materials, disclocation dynamics, finite element analysis, multiaxial fatigue, etc. are reviewed and discussed in Ref. [29]. The multiaxial high-cycle fatigue criteria (MHCF), which are recently developed are based on different theories. They allow to predict the most dangerous points, in which a cracks can initiate and in many cases the orientation of the critical plane and fatigue life to crack initiation or failure. Instead of it seems to be reasonable to perform the theoretical fatigue analysis of subsurface crack initiation in the rolling elements using MHCF hypotheses.

HIGH CYCLE FATIGUE CRITERIA

A general idea of the MHCF criteria is to reduce the complex and multiaxial stress state to an equivalent simple state or a damage scalar factor. They are based on different theories: the critical plane in which stresses results in fatigue failure [5, 14], stress or strain invariants as measures of fatigue load [4], energy formulations estimating the fatigue strength [17] or generalized extensions of empirical results [32]. They require only popular fatigue tests (in many cases only the fully reversed bending and the fully reversed torsion) for investigated material and can be easily adopted to fatigue life analysis of element working in rolling contact conditions such as roller bearings. However, such criteria are clearly less universal than the hypotheses of static endurance. Generally, MHCF criteria are proposed for particular materials or specific loading conditions. Because of this, the selected criteria for a particular material and/or loading (proportional or non-proportional) of calculated machine components require experimental verification. Therefore, if we do not have clear suggestions, it is reasonable to apply a few popular criteria and to compare their results. The problem of sub-surface RCF is often investigated using Dang Van [2, 3, 5, 6], Papadopoulos [2], Liu & Mahadevan [14] criteria.

The criterion proposed by Crossland [4] is among the oldest and the simplest multiaxial high-cycle fatigue criteria and belongs to the hypotheses based at the stress or strain invariants. The invariant formulae concerning the influence of the maximal value of hydrostatic $\sigma_{H,max}$ (the first stress invariant) and the octahedral stresses with the formula:

$$\tau_C = \frac{1}{\sqrt{3}}\sigma_{vM,a} + \left(\frac{3t_{-1}}{f_{-1}} - \sqrt{3}\right)\sigma_{H,\max} \le t_{-1}\,. \tag{5}$$

The use of this hypothesis allows one to determine the initiation point of fatigue cracks. However, the orientation of potential cracks using these criteria cannot be defined.

The Dang Van criterion [5], which is often used in the rolling contact fatigue purposes assumes that the compression effects close microcracks, what is profitable in fatigue mechanism of materials. It leads to adequate decrease of equivalent fatigue stress of structures working in high compression conditions [2, 6]. Because of this, the modification of the DV's criterion, in which the influence of compressive stress is neglected, is proposed for RCF applications [23, 24, 27]:

$$\tau_{DVm} = \max_t \left\{ \begin{array}{ll} \tau(t) + \left(\frac{3t_{-1}}{f_{-1}} - 1.5\right)\sigma_H(t) & \text{for} \quad \sigma_H \ge 0 \\ \tau(t) & \text{for} \quad \sigma_H < 0 \end{array} \right\} \le t_{-1}. \tag{6}$$

The Papadopoulos P_1 hypothesis [20] is proposed for hard metals ($0.577 < t_{-1}/f_{-1} < 0.8$) and is based at an average measure of resolved shear stress amplitude:

$$\tau_{P1} = \sqrt{\frac{5}{8\pi^2}\int_{\varphi=0}^{2\pi}\int_{\theta=0}^{\pi}\int_{\chi=0}^{2\pi}\tau_a^2(\varphi,\theta,\chi)d\chi\cdot\sin(\theta)\mathrm{d}\theta\,\mathrm{d}\varphi} + \left(\frac{3t_{-1}}{f_{-1}} - \sqrt{3}\right)\sigma_{H,\max} \le t_{-1}\,, \tag{7}$$

where: τ_a is the amplitude of resolved shear stress τ, appointed for fixed material plane Δ (determined by φ and θ [23]). For determined material plane $\Delta(\varphi, \theta)$ the amplitude of resolved shear stress τ_a is a function of χ.

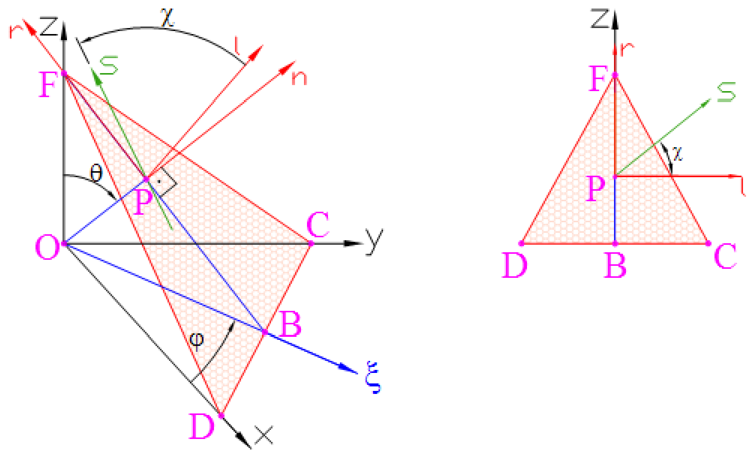

Fig. 2 Orientation of material plane Δ (CDF) crossing point O (points O and P overlap); orientation is defined by two angles: $\Delta(\varphi,\theta)$ and direction of versor **s** on plane Δ is defined by angle χ

The second Papadopoulos P_2 hypothesis (2001) is based on the critical plane approach [21]:

$$\tau_{P2} = \max_{\varphi,\theta}\left(\sqrt{\frac{1}{\pi}\int_{\chi=0}^{2\pi}\tau_a^2(\varphi,\theta,\chi)d\chi}\right)+\left(\frac{3t_{-1}}{f_{-1}}-1.5\right)\sigma_{H,\max} \le t_{-1}, \tag{8}$$

The strain energy hypothesis proposed by T.Łagoda and E.Macha [17] is based on the critical plane approach and distinguishes the strain energy density measure for tension and compression:

$$W_{eqv}^{\max} = \max_t\left(\beta\cdot W_{ns}(t)+\kappa\cdot W_n(t)\right)\le\frac{f_{-1}^2}{2E}, \tag{9}$$

where: W_n and W_{ns} is the normal and shear strain energy density parameter, respectively [17], β and κ are material properties [17].

The fatigue safety factor for all MHCF criteria can be calculated in relation to the admissible value of equivalent fatigue stress with the below formula:

$$x_z = \frac{\text{right hand side of criterion}}{\text{the maximal value of left hand side of criterion}}. \tag{10}$$

Verification of the above criteria for different materials (hard steel, mild steel, cast iron) and loadings (e.g. in-phase and out-of-phase banding plus torsion, multiaxial loading including torsion and high compression) can be found in Ref. [2, 14, 20, 21, 27].

Due to the analysis of RCF of roller bearings using MHCF criteria, the distribution of stresses in function of time must be calculated. The calculations of contact and subsurface stresses can be performed using finite element method - FEM (e.g. ANSYS) or analytical solutions for line contact [22] and elliptical contact [28] based at the Hertz theory [13]. Using the numerical modeling with FEM it is possible to calculate the stresses in any points for different loading conditions, including friction effects and nonlinearity of materials (e.g. plasticity). On the other hand, the analytical solutions based at the Hertz theory are restricted by some assumptions [13]. The most important of them is that the surfaces are frictionless and material must be considered as perfectly elastic.

THE SPHERICAL ROLLER THRUST BEARING

Spherical thrust roller bearings are frequently used in industries such as metalworking, plastics, marine, industrial gearboxes, material handling, mining and constructions. The load is carrying by a spherical barrel-shaped (Fig. 3a) or hour-glass shaped rollers (Fig. 3b). Thus, the possible co-axiality deviations of the supporting bearings as well as shaft bending can be compensated. The preferred geometric relationship between the radii in spherical roller bearings as follows:

(i) with barrel-shaped rollers:

$$R_{r2} < R_o < R_{r1} < R_i, \tag{11}$$

(ii) with hour-glass shaped rollers:

$$R_i < R_{r2} < R_o < R_{r1}, \tag{12}$$

where: R_{r1} and R_{r2} are the maximum and the minimum radius of curvature of the roller profile, respectively, R_o and R_i – is the radius of curvature of the outer and inner raceway, respectively.

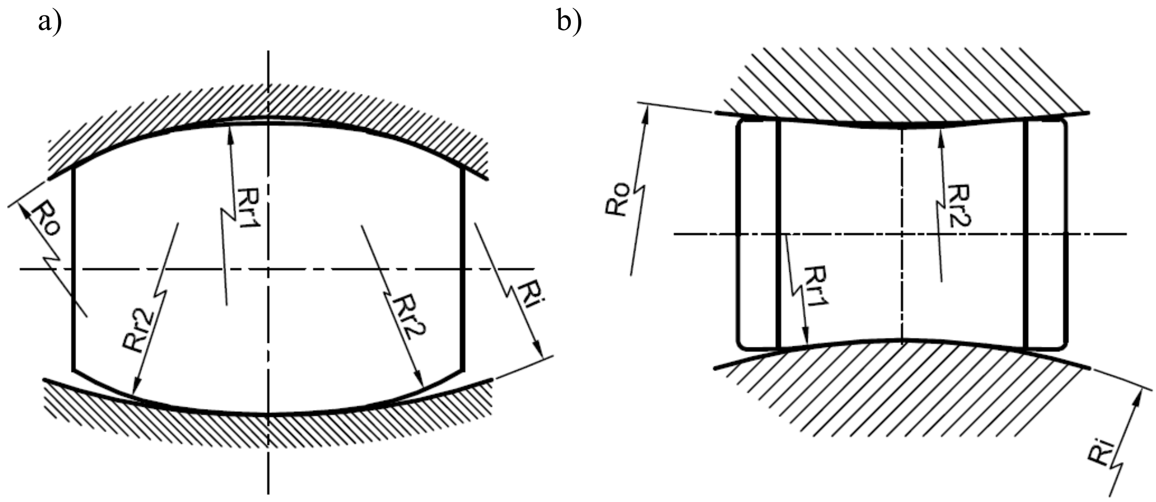

Fig.3 barrel-shaped (at left hand-side) and hour-glass shaped (right hand-side) spherical rollers

The load is transmitted by a barrel from one raceway to the other at an angle to the bearing axis. Therefore, they are primarily intended for axial (thrust) loads, although they can carry combined loads, in which additional external radial load should not exceed 50-55% of the simultaneously acting axial load. They are internally self-aligning and they can operate at very high axial loads and relatively high speeds. Some information about experimental wear and fatigue life of lubricated spherical roller thrust bearing can be found in Ref. [18, 19].

The fatigue analyses using FEM and selected MHCF were performed for a spherical thrust roller bearing designated as 293/1600EF [33]. The most important information, such as principal dimensions, basic load ratings and fatigue load limit on the investigated roller bearing, are presented in Table 1. This bearing is perfectly suited for heavy duty applications with axial loads or combined axial and radial loadings. The exemplary machine with the bearing arrangement including the investigated spherical roller thrust bearing is a very large tunnel boring machine – TBM, designated as the Mk 27 [1]. This machine with spans a diameter range of 6.5 to 12.5 meters develops a thrust loading of up to 19000 kN [1]. It should be noted, that the thrust load carried by the investigated bearing in above application greatly exceeds the fatigue load limit F_u = 11800 kN given by the manufacturer (Table 1).

Table 1 The dimension and load ratings of investigated spherical roller thrust bearing 293/1600EF [33]

Designation	Principal dimensions			Basic load ratings		Fatigue load limit
				dynamic	static	
	d	*D*	*H*	*C*	C_0	F_u
	mm			kN		kN
293/1600EF	1600	2280	408	36800	200000	11800

Using mathematical and numerical FEM calculation with application of MHCF criteria it is possible to perform parametric optimization of the raceway and barrel radii including real stress and strain distributions in cooperating elements. The optimal selection of such radii has a significant influence at the maximal fatigue load limit and the fatigue life of roller bearing.

The detailed information on rolling bearings, such as a barrel and raceways radii, are not provided by manufacturers. For this reason, more unfavorable a one-point contact between rolling element and rings was assumed in the numerical model. The calculations of subsurface stresses and fatigue effort were performed for different contact conditions with various radii R_{r1} of spherical barrel-shaped roller element contact surface. The radius of inner and outer rings contact surfaces were set to R_i=R_o = 1580 mm. The radius of the roller element was assumed in the range of R_{r1}=R_{r2} = {1545; 1580} mm (see Fig. 3).

The calculations of subsurface stresses were performed using finite element method (ANSYS). The structural high-order 3D solid (SOLID95) and contact elements (CONTA174) were used in the calculations. The finite element mesh was irregular with strong concentration of regular hexahedral elements in the contact area (Fig. 4). Furthermore, the rolling friction coefficient μ = 0.0018 was adopted in the investigated numerical model. The axial load F_a acting in the axis of symmetry of the bearing and equal to the fatigue load limit F_u =11800 kN suggested by the producer [33] was adopted. The thrust force of one roller element was assumed as follows:

$$F_z = \frac{F_u}{z} = 393{,}3 \text{ kN} \tag{13}$$

where z = 30 is the number of rolling element in the bearing.
Due to the symmetry, only a half part of rolling element was modeled (Fig. 4). The problem was calculated in two steps: (i) full model (Fig. 4a), and (ii) submodel, for subsurface stress calculation (Fig. 4b).

In order to perform fatigue analysis, it was assumed that both rings and rolling elements are made from the same material X105CrMo17 [33] with chemical composition given in the Table 2. Some material properties of this stainless steel with high chromium content are given in Table. 3. The values of the fully reversed bending and torsion fatigue limit for number of cycles to fatigue N = 10^8 were estimated on the basis of the tensile strength. However, it should remember that bearing steel does not have ant fatigue limit [31].

Table 2. Chemical composition of X105CrMo17

Cr %	C %	Mn %	Si %	P %	S%	Mo %
16÷18	0.95÷1.20	< 1	< 1	< 0.04	< 0.03	< 0.75

The distribution of the equivalent von Mises stress in the spherical roller thrust bearings with the roller radius R_{r1} = R_{r2} = 1545 mm, designated as 293/1600EF, for maximal fatigue load limit F_u given in catalogue is presented in Fig. 5. In the second example, the roller element has the same radius as inner and outer rings contact surfaces. It results in increasing of the maximal contact pressure at the contact edge (Fig.6). Moreover, the equivalent von Mises subsurface stress σ_{vm} achieves large values in such conditions (Fig.7). The same problem occurs in the cases of slight differences between the raceway R_i=1580 mm and roller element ($R_{r1} = R_{r2}$ = {1577; 1580} mm) radii.

Table 3. Material properties of steel X105CrMo17 after heat-treatment [27]

Parameter	E	σ_y	σ_f	Hardness	f_{-1}	t_{-1}
Value	$2{,}23 \cdot 10^5$ MPa	1635 MPa	1780 MPa	56 HRC	712 MPa	427 MPa

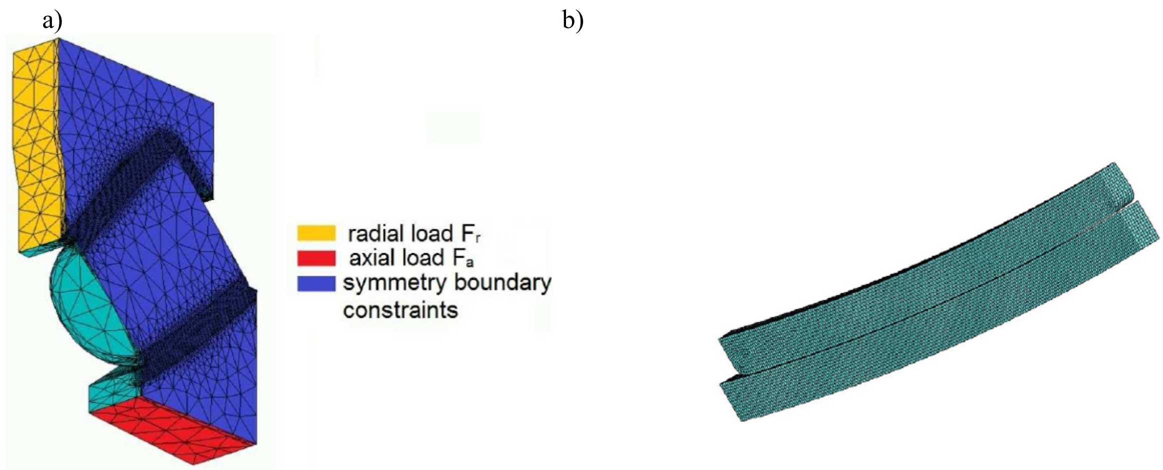

Fig. 4. Numerical FEM model of spherical thrust roller bearing (293/1600EF)
a) coarse (full) model
b) submodel of contact region

Larger differences between roller and raceway radii ($R_{r1} = R_{r2}$ = {1545; 1550; 1560} mm) results in significant changes of the contact and the subsurface stress distributions. The maximal von Mises stress in these cases occurs below a few millimetres below the center of the contact area (Fig. 5). These maximal values of σ_{vm} are much smaller than for $R_{r1} > 1575$ mm (Table 4).

The values of the fatigue safety factor calculated using MHCF criteria are presented in the Table 5. Such criteria requires only popular fatigue tests (fully reversed bending and torsion) for investigated material and can be easily adopted to fatigue analysis of roller bearings. However, not all the criteria are applicable in RCF [2, 6, 23-27]. The application of popular Dang Van (DV) hypothesis results in underestimation of the equivalent fatigue stress (Table 5) of elements working in rolling contact conditions [23, 24]. Therefore, the modification of the original Dang Van (DV_m) formula was used [23]. In all cases the most dangerous points were below the surface close to the radius of P-L points.

The difference of the fatigue effort calculated using P_1 hypothesis in relation to other criteria is caused by not taking into account the effect of shift in phase between the normal and shear stresses in the criteria based at integral formulation (e.g. P_1). This result confirms with the experimental tests for the notched specimens. However, in the case of rolling contact the concentration of stresses is not caused by a notch and cracks initiation below the surface [27]. Therefore, to determine the influence of three-dimensional compression with non-proportional shear on the subsurface fatigue, special tests including this kind of loading should be performed. Hence, if there are no experimental tests including the stress state in elements working in rolling contact conditions, it is reasonable to use criteria based on integral approach such as P1, which gives the most conservative results.

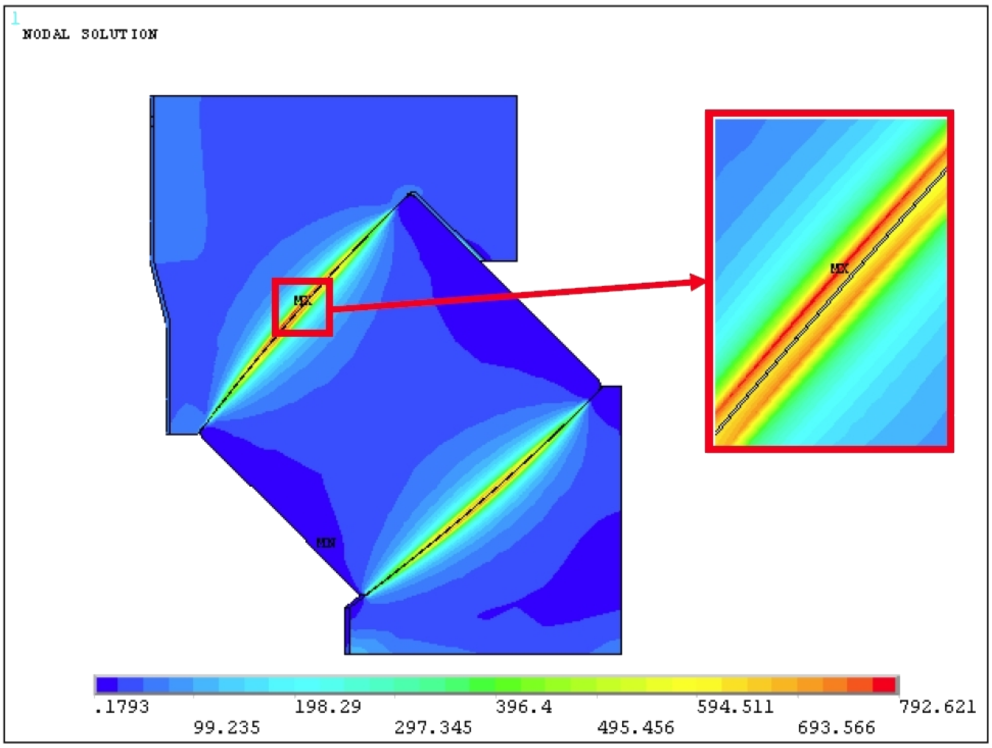

Fig.5 Equivalent von Mises stress $\sigma_{vM(MAX)}$ = 793 MPa, radius of roller element R_{r1} = 1545 mm

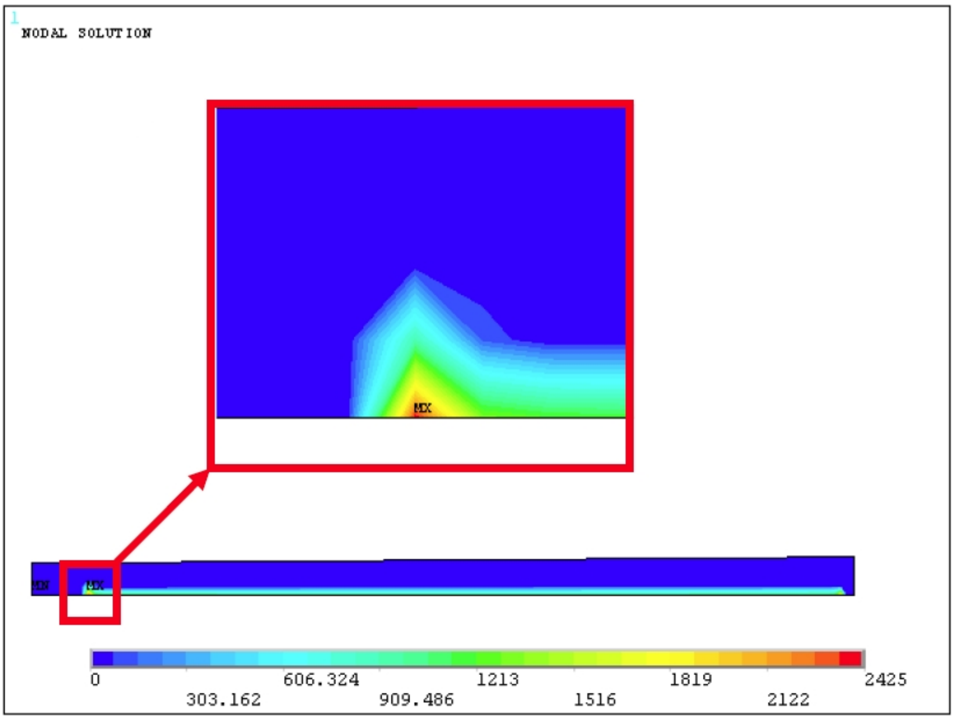

Fig. 6. Concentration of high contact stresses at the edge of the contact caused by the same profiles of barrel and raceway

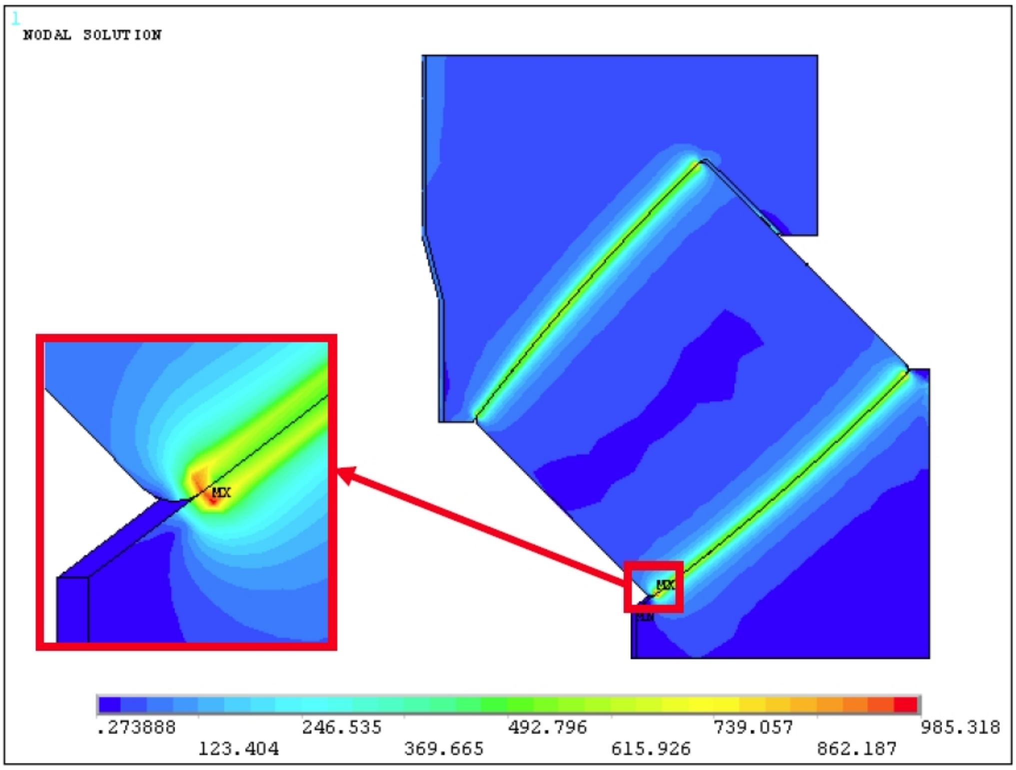

Fig.7 Equivalent von Mises stress $\sigma_{vM(MAX)}$ = 985 MPa, radius of roller element R_{r1} = 1580 mm

The performed fatigue analysis using the presented MHCF criteria suggest that the most optimal is the radius R_{r1} = 1560 mm. In this case the smallest von Mises (Table 4) and the equivalent fatigue stresses were obtained (Table 5). The maximal fatigue load using MHCF criteria and classical P-L model (1) given in ISO standard [12] for assumed number of cycles to failure and assumed the optimal radius of the barrel curvature R_{r1} = 1560 mm were calculated and presented in the Table 6. The P_1 hypothesis gave the closest solution to the admissible fatigue load limit F_u suggested by the producer. However, the fatigue life L calculated using P-L relationship (1) is about L_{10}=40 million revolutions for this loading, what corresponds to $N = 10 \cdot 10^8$ stress cycles to failure in roller elements. In engineering application the rating life L_{10} for rolling bearings is often assumed to be about 10 million revolutions. On the other hand, the fatigue life for the maximal admissible fatigue loading calculated using the remaining criteria (D_{vm}, P_2, E) was between $L = 10 \div 13 \cdot 10^6$ revolutions.

The more detailed analysis about engineering application, contact and subsurface stress distribution analysis of the presented spherical thrust roller bearing is presented and discussed in Ref. [25].

Table 4. The maximal contact pressure and the maximal von Mises stress in the spherical roller thrust bearing for different radius of curvature of the roller profile R_i=R_o=1580 mm, F_u=11800 kN.

		Radius of curvature of the roller profile R_{r1}=R_{r2} mm				
		1580	1577	1560	1550	1545
p_o MPa	roller	2015	2170	1578	1584	1592
σ_{vM} MPa	raceway	834	902	693	762	793
	roller	947	1002	684	716	732

Table 5. The estimated values of the safety factor x_z in the spherical roller thrust bearing for various roller element radius, material X105CrMo17

radius of roller element mm	The safety factor x_z					
	Dang Van	Modified Dang Van DV_m	Papadopoulos P_1	Papadopoulos P_2	Crossland C	Łagoda E
R_{r1} = 1545	1.69	1.16	0.98	1.16	1.08	1.14
R_{r1} = 1550	1.74	1.20	1.00	1.20	1.11	1.18
R_{r1} = 1560	1.83	1.30	1.04	1.30	1.14	1.26

Table. 6. The maximal fatigue axial loading F_u' for different MHCF criteria, R_{r1} = 1560 mm, material X105CrMo17, spherical roller thrust bearing 293/1600EF, catalogues fatigue life limit F_u = 11800 kN

criterion	D_{vm}	P_1	P_2	C	E	F_u =11800 kN	comments
$F_u' \cdot 10^3$kN	18	12	18	15	17	11.8	
F_u'/F_u	1.5	1.0	1.5	1.2	1.4	1.0	
L_{10} mln rev.	10.8	41.9	10.8	19.9	13.1	44.3	P-L (eq. 1)
N (roller element)	$2.5 \cdot 10^8$	$9.5 \cdot 10^8$	$2.5 \cdot 10^8$	$4.5 \cdot 10^8$	$3 \cdot 10^8$	$10 \cdot 10^8$	number of cycles to failure

THE CYLINDER ROLLER THRUST BEARING

The cylindrical roller bearings are simpler in form and design that spherical roller bearing. They have low friction torque characteristics and they are suitable for high-speed operation. Due to this fact, they are typically used in machine tools, transmissions, vibration machines and rail vehicles. Both radial and axial cylindrical roller bearing can accommodate heavy loads radial and axial, respectively. The thrust bearing are also relatively insensitive to shock loads and require little axial space. However, incorrect profiles of roller and raceway surfaces of the cylindrical roller bearing can leads to increase of the surface and subsurface stresses at the end of the contact (Fig. 8). These stresses can tend to large values (theoretically and numerically tends to infinity) when perfectly straight roller is in contact with the raceway of the same profile (Fig. 8a). It is caused by tension stresses under the non-loaded part of raceway, which tries to restore the undeformed state. Such effects are not included in theoretical Hertz solution. The problem of the stress concentration at the edge of a roller element can be reduced or eliminated by some techniques presented in Fig. 8b. Because of this, it is necessary to analyze the cross sectional shape of the bearing track and roller element.

a) b)

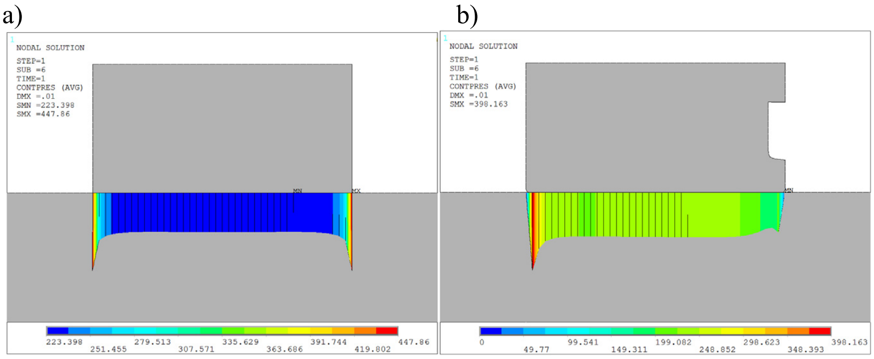

Fig. 8 High contact stress concentration at the edge of the cylindrical roller and method of their elimination
a) cylindrical roller without round head
b) cylindrical roller with round head at left hand-side and with stiffness reduction by removing material at the front of the roller at right hand-side

Typically, the roller elements have a partially crowned (barrel) type shape to avoid the concentration of contact stresses at the edge of roller. The crowning of rollers, with radius $r_r/d \approx 2$ or logarithmic diminishment with rounded corner (Fig. 9) [7], also gives the bearing protection against the effects of slight misalignment. The roller profile has a significant influence at the contact stress distribution between roller and raceway.

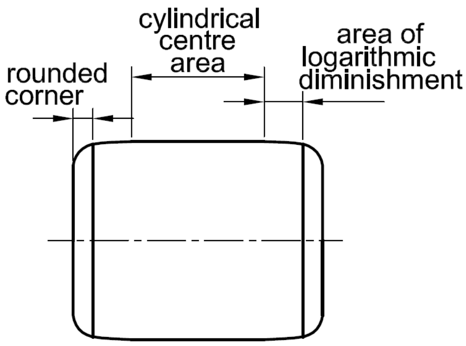

Fig. 9 The cylindrical roller with rounded corner

The fatigue analyses were performed for the cylindrical roller thrust bearing designated as K 81220 TN [33]. The principal information, including fatigue load limit given by manufacturer, are presented in the Table.7. The roller element, which was assumed in the presented numerical model (Fig. 10) does not had a round head. In such case the concentration of the contact pressure at the edge of the contact occurs in the form presented in the Fig. 8a. However, the stress distribution in the mid-part (Fig. 11) was convergent with the 2-D model with plane strain assumption and theoretical models [22, 13]. The irregular mesh with strong concentration of regular hexahedron elements (SOLID95) in the area of high stresses was used in the numerical model (Fig. 10). The roller elements used in roller bearings have rounded head and often logarithmic profiles. Due to this fact it is important to include the effective length of the contact between roller and raceway. In order to take into account the rounded and logarithmic diminishment part of the cylindrical roller the effective length of the contact L_{eff} was defined with the formula:

$$L_{eff} = \frac{\text{contact length}}{\text{length of roller element}} \cdot 100\%, \tag{14}$$

where the length of the cylindrical roller was equal to 11 mm.

Two cases with the L_{eff} = 100% and L_{eff} = 73% were investigated in the paper. The values of the fatigue safety factor for assumed contact conditions are presented in the Table 8. The obtained results (Table 8 – the safety factor and Table 9– the maximal fatigue axial load) have the same tendency as for spherical roller thrust bearing. The maximal fatigue axial load for the contact length equal to L_{eff} = 73% of the roller length was in the range of F_u' = 55 ÷ 91 kN (F_u = 62 kN). Using the P_1 criterion the most conservative result was obtained and the maximal load for this hypothesis was equal to $F_u' = 0.9 \cdot F_u$.

Table 7 The dimension and load ratings of investigated cylindrical roller thrust bearing K 81220 TN [33]

Designation	**Principal dimensions**			**Basic load ratings**		**Fatigue load limit**
				dynamic	**static**	
	d	*D*	*H*	*C*	C_0	F_u
	mm			kN		kN
K 81220 TN	100	135	25	156	630	62

a) b)

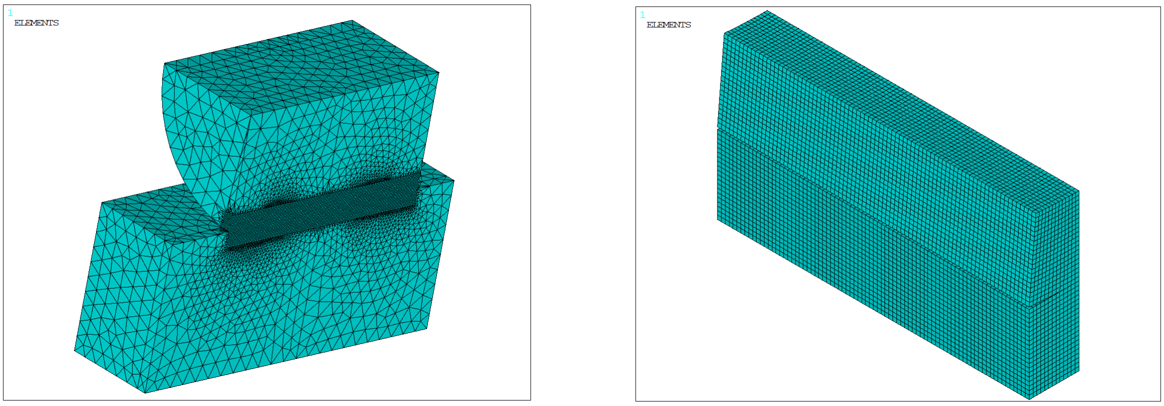

Fig. 10 The numerical model of the cylindrical thrust roller bearing
a) full-model
b) mesh in the high stress area

a) b)

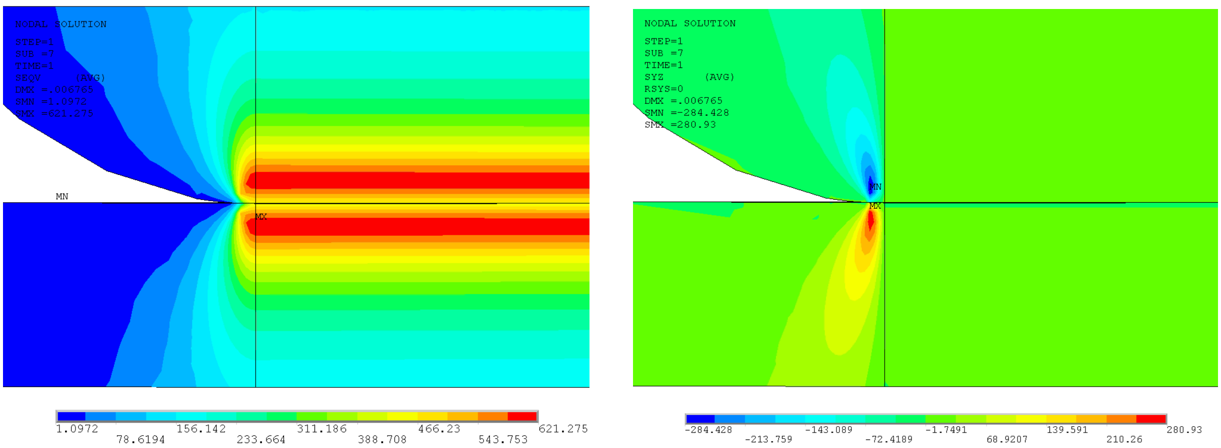

Fig. 11. Subsurface stress distribution in the cross-sections of the cylindrical roller bearing,
a) the equivalent von Mises stress $\sigma_{vm(MAX)}$ =621MPa
b) the shear stress with the maximal values in the P-L point at the right hand-side $\tau_{xy(MAX)}$ = 281 MPa

Table 8. The estimated values of the safety factor x_z in the cylindrical roller thrust bearing for various roller element radius, material X105CrMo17

L_{eff} [%]	The safety factor x_z			
	Crossland C	Modified Dang Van DV_m	Papadopoulos P_1	Papadopoulos P_2
100%	1.37	1.42	1.11	1.29
73%	1.17	1.21	0.94	1.10

Table 9. The maximal fatigue axial loading F_u' for different MHCF criteria, material X105CrMo17, cylidrical roller thrust bearing, catalogues fatigue life limit Fu = 62 kN (contact length equal to 73% of the roller length was assumed)

criterion	DV_m	P_1	P_2	C	F_u =62 kN	comments
$F_u' \cdot 10^3$ kN	91	55	75	86	62	
F_u'/F_u	1.5	0.9	1.2	1.4	1.0	
L mln rev.	6.0	32.3	11.5	7.3	21.7	P-L (eq. 1)

RESULTS AND CONCLUSIONS

Ball and roller bearings have been subjected to the most extensive experimental rolling fatigue testing of all components working in contact condition. The information about the basic load ratings and sometimes fatigue load limit based on fatigue failure consideration are given in catalogues. However, it is assumed that bearings does not have unlimited life. The application of proposed mathematical models in current norms may require expensive and time consuming RCF endurance testing. In such case, the application of MHCF criteria it seems beneficial. The expensive and time consuming rolling contact fatigue testing of bearings are not necessary in context of application of such criteria. However, not all proposed MHCF models are applicable in the RCF of bearings.

The performed calculations for spherical and cylindrical roller bearings show that the criteria based at integral formulation (e.g. P_1) gives more conservative results. However, the results obtained using P_1 criterion may be overestimated due to neglecting the shift in phase between stresses, which is very important in the rolling contact phenomena. The other investigated criteria based on different approaches gave similar results in both cases. Furthermore, the results obtained using above criteria was in good agreement with fatigue load limits proposed by manufacturers for both investigated problems.

The presented methodology of determination of the safety factor, or in many cases, the fatigue life prediction can be easily adopted to radial roller bearings and also for gears, rails, railway wheels and other elements working at rolling contact conditions.

REFERENCES

[1] Bergling G., Forsberg J., Hartwig S., Wohiwend K.: Main Bearings for Advanced TBMs. Proceedings – Rapid Excavation and Tunneling Conference, 1995, pp. 493 – 508.
[2] Bernasconi A., Filippini M., Foletti S., Vaudo D.: Multiaxial fatigue of a railway steel under non-proportional loading, International Journal of Fatigue, 2006, 28, p. 663–672.
[3] Ciavarella M., Monno F., Demelio G.: On the Dang Van fatigue limit in rolling contact fatigue, International Journal of Fatigue, Vol. 28, 2006, pp. 852–863.
[4] Crossland B.: Effect of large hydrostatic pressures on the torsional fatigue strength of an alloy steel, Proc. Int. Conf. Fatigue of Metals, London, 1956, pp. 138–49.
[5] Dang Van K., Maitournam M. H.: On some recent trends in modelling of contact fatigue andwear in rail, Wear, Vol. 253, 2002, pp. 219–227.
[6] Desimone H., Bernasconi A., Beretta S.: On the application of Dang Van criterion to rolling contact fatigue, Wear, Vol. 260, 2006, pp. 567–572.
[7] DIN 5402
[8] Ekberg A., Kabo E.: Fatigue of railway wheels and rails under rolling contact and thermal loading – an overview, Wear, Vol. 258, 2005, pp. 1288–1300.
[9] Ekberg A.: Rolling contact fatigue of railway wheels – a parametric study, Wear, Vol. 211, 1997, pp. 280-288.
[10] Ioannides, E., and Harris, T. A.: A New Fatigue Life Model for Rolling Bearings, ASME J. Tribol., Vol. 107, 1985, pp. 367–378.

[11] Ioannides, E., Bergling, G., and Gabelli, A.: An Analytical Formulation for the Life of Rolling Bearings, Acta Polytech. Scand., Mech. Eng. Ser., Vol. 137, 1999, pp. 58–60.
[12] ISO: Rolling Bearings—Dynamic Load Ratings and Rating Life, Draft International Standard ISO/DIS, 281, 1989, ISO, Geneva, Switzerland.
[13] K. L. Johnson: Contact mechanics, Cambridge university press, 2004.
[14] Liu Y., Stratman B., Mahadevan S.: Fatigue crack initiation life prediction of railroad wheels, International Journal of Fatigue, Vol. 28, 2006, pp. 747–756.
[15] Lundberg, G., and Palmgren, A.: Dynamic Capacity of Rolling Bearings, Acta Polytech. Scand., Mech. Eng. Ser., Vol. 1 (3), 1947, pp. 1–52.
[16] Lundberg, G., and Palmgren, A.: Dynamic Capacity of Roller Bearings, Acta Polytech. Scand., Mech. Eng. Ser., Vol. 2 (4), 1952, pp. 96–127.
[17] Łagoda T., Energy models for fatigue life estimation under uniaxial random loading. Part I: The model elaboration, International Journal of Fatigue, Vol. 23, 2001, pp. 467–480.
[18] Olfsson U.: An experimental investigation of wear and fatigue life reduction of boundary lubricated spherical roller thrust bearings, Tribology International Vol. 30, No. 9, 1997, pp. 685–692.
[19] Olfsson U.: Characterisation of wear in boundary lubricated spherical roller thrust bearings, Wear 208, 1997, pp. 194-203.
[20] Papadopoulos I.V., Davoli P., Gorla C., Filippini M., Bernasconi A.: A comparative study of multiaxial high-cycle fatigue criteria for metals, International Journal of Fatigue vol.19 no. 3, 1997, pp. 219-235.
[21] Papadopoulos I.V.: Long life fatigue under multiaxial loading, International Journal of Fatigue, Vol. 23, 2001, pp. 839–849.
[22] Radzimovsky E. I.: Stress distribution and strength condition of two rolling cylinders pressed together, University of Illinois Bulettin, Vol. 50, No. 44. 1953, pp. 1-40.
[23] Romanowicz P.: Application of selected multiaxial high-cycle fatigue criteria to rolling contact problems. Key Engineering Materials, Vol. 542, 2013, pp. 157-170.
[24] Romanowicz P.: Kryteria zmęczenia wysokocyklowego w zastosowaniu do zagadnień kontaktu tocznego, Czasopismo Techniczne, Vol. 3-M/2011, 2011, pp. 75-91 [in Polish].
[25] Romanowicz P.: Analiza wysokocyklowego wytężenia zmęczeniowego łożyska baryłkowego, Przegląd Mechaniczny, Vol. 11/12, 2012, pp.17-24 [in Polish].
[26] Romanowicz P., Zieliński A. P.: Wieloosiowe zmęczenie elementów pracujących w warunkach kontaktu tocznego, Acta Mechanica et Automatica, Vol. 3, no. 2, 2009, pp. 86-88 [in Polish].
[27] Romanowicz P.: Fatigue analysis of selected machine elements working at rolling contact condition, PhD Thesis, Cracow University of Technology, Cracow 2010 [in Polish].
[28] Sackfield A., Hills D. A.: Some useful results in the classical Hertz contact problem, Journal of Strain Analysis, Vol. 18, No. 2, 1983, pp. 101- 105.
[29] Sadeghi F., Jalalahmadi B., Slack T. S., Raje N., Arakere N. K.: A Review of Rolling Contact Fatigue, Journal of Tribology, Vol. 131, 2009, 041403.
[30] Schlicht, H., Schreiber, E., and Zwirlein, O.: Fatigue and Failure Mechanism of Bearings, I Mech E Conf. Publ., Vol. 1, 1986, pp. 85–90.
[31] Shimizu, S.: Fatigue Limit Concept and Life Prediction Model for Rolling Contact Machine Elements, Tribol. Trans., Vol. 45 1, 2002, pp. 39–46.
[32] Weber B., Fatigue multiaxiale des structures industrielles sous chargement quelconque [En ligne] Thèse : Institut National des Sciences Appliquées de Lyon, 1999.
[33] http://www.skf.com.